Electrochimica Acta 182 (2015) 1118–1123

Contents lists available at ScienceDirect

Electrochimica Acta

journal homepage: www.elsevier.com/locate/electacta

Soluble TTF catalyst for the oxidation of cathode products in Li-Oxygen battery: A chemical scavenger

Walter R. Torres, Santiago E. Herrera, Alvaro Y. Tesio, María del Pozo, Ernesto J. Calvo*

INQUIMAE Facultad de Ciencias Exactas y Naturales, Universidad de Buenos Aires. Pabellon 2, Ciudad Universitaria, AR-1428 Buenos Aires, Argentina

ARTICLE INFO

Article history:
Received 10 June 2015
Received in revised form 14 August 2015
Accepted 22 September 2015
Available online 9 October 2015

Keywords:
tetrathiafulvalene
lithium air batteries
soluble catalyst
ORR, redox titration

ABSTRACT

One of the challenges for the success of electric vehicles is to achieve a non aqueous Li-O_2 battery efficient in the oxidation of solid Li_2O_2 during battery charging. Bruce et al. have proposed that soluble tetrathiofulvalene (TTF) in the electrolyte, makes it possible to recharge the battery at high current densities and low over-potential. We disclose here a detailed study of Li_2O_2 and solvent degradation products oxidation on gold electrode in 0.1 M $LiPF_6$ DMSO electrolyte with soluble TTF using a variety of techniques: rotating ring disk electrode (RRDE), scanning electrochemical microscopy (SECM), electrochemical quartz crystal microbalance (EQCM) and atomic force microscopy (AFM). The experimental evidence demonstrates that it is possible recover a clean Au surface using TTF as a soluble catalyst that titrates the surface products formed during the O_2 reduction.

1. Introduction

The rechargeable Li-O_2 battery exhibits a very large theoretical energy density that can compete with fossil fuels for electric vehicle applications with extended mileage range [1–4]. The non aqueous Li-O_2 battery introduced in 1996 by Abraham [1], consists of a lithium metal anode that dissolves in non aqueous electrolyte and the resulting Li^+ ions react with oxygen reduction products to form insoluble lithium peroxide, Li_2O_2, at a porous carbon cathode during discharge. Since the product is insoluble, the electrode kinetics of the oxygen reduction reaction (ORR) in lithium air battery cathodes strongly depends on the solvent [5–7], electrolyte cation [8] and electrode material [9]. On carbon and gold electrodes the first ORR product, superoxide, is stable in non aqueous solutions containing tetralkyl ammonium cations, but in lithium containing solutions soluble LiO_2 can disproportionate or undergo further reduction to insoluble Li_2O_2.

Among non aqueous solvents, dimethyl sulfoxide (DMSO) with a very large dipole moment and the appropriate geometry to coordinate Li+ ions has been recently proposed for rechargeable Li-O_2 batteries [10]. Peng et al. have shown that the Li-O_2 battery can be recharged with 95% capacity retention in 100 cycles using DMSO electrolyte and porous gold electrode [11].

One of the major challenges for the non aqueous Li-O_2 battery is the efficient oxidation of solid Li_2O_2 in the porous cathode during battery charging and the large over potential needed to oxidize Li_2O_2 into O_2 and Li^+ [12] arises from the non conducting solid. Depending on the experimental condition large Li_2O_2 toroidal particles can be formed which are hard to oxidize at low potential.

There is also a controversy on the stability of DMSO in the presence of oxygen reduction reaction (ORR) products [13] which becomes more evident when the electrode area to electrolyte volume is high [14]. McCloskey et al. have shown that the balance of O_2 consumed in the ORR and that evolved in the OER during charging is always less than 0.9 [13]. Thus, while the ORR is a 2-electron process, further heterogeneous chemical reaction of the solid peroxide with the electrolyte or the carbon cathode decreases the amount of peroxide on the surface so that the outermost surface of Li_2O_2 can react chemically with the solvent and/or the electrolyte and the side reaction products make difficult the recharge.

Furthermore, above 4.2 V DMSO is electrochemically oxidized to dimethyl sulfone on Au so that it is imperative to reduce the charging overpotential by using a catalyst [15].

Bruce and co-workers have shown that incorporating soluble TTF redox mediator in the electrolyte, it is possible to recharge the battery at high current densities and low overpotential [16].

In the soluble mediator strategy the redox potential of the soluble mediator should be slightly higher than the equilibrium potential of the O_2/Li_2O_2 reaction, i.e. 2.96 V. The oxidized form of the redox catalyst should be capable of efficiently decomposing Li_2O_2 and the reduced form should be oxidized at the electrode surface uncovered by the non conducting lithium peroxide.

* Corresponding author. Tel.: +5411 4576 3378; fax: +5411 4576 3341.
E-mail address: ernestojulio.calvo@gmail.com (E.J. Calvo).

http://dx.doi.org/10.1016/j.electacta.2015.09.130
0013-4686/

Another requirement for the soluble redox mediator is that it must not react with electrolyte/solvent or the Li metal anode.

Several soluble redox couples have been proposed, including tetrathiafulvalene (TTF/TTF^+) [16,17], ethyl viologen [18–20] and tri-iodide (I_3^-/I_2) [21]. A dual catalyst combining ethyl viologen and LiI has been recently discussed [22] and also a bifunctional catalyst of soluble Fe phtalocyanine shuttles electrons both in the cathodic and anodic reactions [23]. Zecevic et al. filed a patent on the use of soluble redox oxygen evolving catalysts [24].

The electrochemistry of TTF in DMSO exhibits two one-electron reversible waves with half wave potentials at 3.65 V and 3.87 V respectively according to the following reactions:

$$TTF \rightarrow TTF^+ + e \quad (1)$$

$$TTF^+ \rightarrow TTF^{2+} + e \quad (2)$$

In the present article we explore the interaction of the insoluble Li_2O_2, and other ORR side products with soluble TTF^+ in DMSO containing lithium ions, using a variety of electrochemical techniques (RRDE, AFM, EQCM and SECM). In RRDE the soluble TTF^+ and TTF^{2+} can be collected and measured at an Au ring electrode of a rotating ring disc electrode (RRDE) system at 3.0 V by reduction under convective-diffusion conditions. If these soluble redox species react with solid Li_2O_2, less collection current would be detected at the ring so the redox mediator reaction can be followed quantitatively. The electro-chemical quartz crystal microbalance (EQCM) measures the mass increase of insoluble ORR products and the surface mass loss by redox titration of Li_2O_2 by TTF^+ shuttling electrons to the underlying electrode. Finally, the SECM experiment assesses the ability of soluble TTF^+ to oxidize the insoluble blocking ORR products at the tip electrode from the solution by chemical reaction.

With the combination of techniques we show that the action of TTF^+ is to decrease the O_2 battery cathode oxidation overpotential and to explain the mechanism of surface species scavenging.

2. Experimental Section

2.1. Reagents

Anhydrous dimethyl sulfoxide (DMSO) ≥99.9% (SIGMA–ALDRICH), lithium hexafluorophosphate battery grade, ≥99.99% trace metals basis (ALDRICH), were stored in the argon-filled MBRAUN glove box with the oxygen content ≤0.1 ppm and water content below 2 ppm. DMSO was dried for several days over 3 Å molecular sieves, (SIGMA–ALDRICH); all solutions were prepared inside of the glove box and the water content was measured using the Karl Fisher 831 KF Coulometer (Metrohm). Solutions were found to contain initially around 50 ppm of water.

2.2. Techniques and procedures

2.2.1. Reference and counter electrode

The reference electrode was a Pt wire coated with a $LiMn_2O_4$/$Li_2Mn_2O_4$ [25]. The reference electrode was calibrated with respect to Li/Li^+ couple, that is commonly used as reference in Li-air battery studies. Inside the argon glove box, a $LiMn_2O_4/Li_2Mn_2O_4$ electrode and a 3.2 mm diameter Li wire (99.9% trace metals basis ALDRICH) were placed in a beaker filled with 0.1 M $LiPF_6$ in DMSO and the cell potential was measured with a high impedance voltmeter obtaining 3.25 V.

The auxiliary electrode used in all the experiment was a Pt gauze (Good-fellow PT008710/43).

2.2.2. Rotating ring disk electrode measurement (RRDE)

RRDE experiments were performed in an air-tight acrylic box filled with Ar and dried with phosphorous pentoxide keeping a positive pressure by a stream of dry oxygen. The motor controller, motor and disk and ring mercury contacts in the bearing block are located outside the air-tight acrylic box and sealed with a rubber ring. The electrochemical cell and RRDE cylinder immersed in the aprotic electrolyte were kept inside the box. This box contained the four-electrode glass cell and the electrolyte was fed from bottles filled in the glove box by a system needles and Teflon tubes without contact with the atmosphere. Large area platinum gauze was used as counter electrode in a compartment separated from the main compartment by a fritted glass.

A GC disk Au ring rotating ring disk electrode embedded in Araldite epoxy resin cylindrical body (Ciba-Geigy) with $r_1 = 0.25$, $r_2 = 0.26$, $r_3 = 0.31$ cm and a 0.196 cm^2 geometric area. The geometric collection efficiency $N_o = 0.32$ was calculated using the Albery–Hitchman theory [26] and experimentally verified with the $Fe(CN)_6^{4/3-}$ redox couple in a galvanostatic experiment. The ring electrode was kept at $E_R = 3.0$ V vs Li/Li^+ in DMSO so that alternatively O_2^- was oxidized while TTF^+ and TTF^{2+} were reduced under convective-diffusion respectively.

2.2.3. Atomic force microscopy (AFM)

For ex-situ AFM experiments, a three electrode EC-AFM electrochemical cell was built using Teflon® and a Kalrez o-ring pressed onto gold sample with a 0.64 cm^2 area. The cell was contained in a glass cylinder environmental chamber filled with dry oxygen. Chronoamperometry experiments were carried out with a potentiostat/ galvanostat coupled with the AFM (EC-AFM, Agilent 5500 AFM /SPM).

The surface was scanned by AFM using an insulating triangular Si tip PointProbe® Plus Non-Contact / Soft Tapping Mode (radius <10 nm force constant 48 N m^{-1}, resonance frequency 157.85 kHz) using non contact mode. In a typical experiment after the electrochemical treatment the surface was rinsed with 10 DMSO aliquots (100 μL) and dried under Ar. Image analysis was performed with Gwyddion 2.33 software (http://hwyddion.net/).

2.2.4. Scanning electrochemical microscopy (SECM)

The electrochemical cell with the sample press fitted at its bottom hole fixed with a Kalrez o-ring was mounted on the three-axis translation stage of a home-built SECM. The system was driven by computer controlled stepper motors with a nominal resolution of 0.6 μm per half step in each direction (OWIS GmbH, Germany). The tip potential was controlled by a bipotentiostat (EI-400 FCV, Cypress Systems, USA). A purpose-built Visual Basic (Microsoft, US) software routine was employed for the control of the SECM, tip positioning, data acquisition and display. Calibrating approach curves were obtained in 1 mM ferrocene–methanol in 0.1 M KCl solution. The SECM tips were insulated in quartz tubing. Disk shaped platinum microelectrodes (5 and 10 μm disk radius) were produced by pulling 25 μm diameter Pt wires (Goodfellow, UK) inside quartz capillaries (Q100-30-15, Sutter Instrument Co., USA) with a laser based pipette puller (P-2000, Sutter Instrument Co., USA). The tip was positioned at a suitable distance from the sample (typically 10–15 μm). Based in surface generation-tip collection mode, TTF^+ was detected in the tip applying an oxidative potential on the gold substrate (3.65 V) and different reductive potential in the tip (3.25 V or 3.00 V).

2.2.5. Electrochemical quartz crystal microbalance (EQCM)

Fast quartz crystal impedance measurements were performed using an ac voltage divider at 10 MHz. A sinusoidal voltage (5 mV peak to peak) generated by a voltage controlled oscillator (VCO) connected to the D/A output of a Keithley Data Acquisition System

575 was applied. Both, the input, V_i and output, *Vo* voltage moduli were amplified (MAX436 rf op. amp.) and rectified with an ideal diode circuit based on an LH0024 operational amplifier. The resulting signals were measured with an A/D converter of the Keithley Data Acquisition System 575. An AT-386 computer generated the perturbing ac signal and was used to calculate the modulus of the circuit transfer function, i.e. Vo/Vi as a function of the VCO output signal frequency. The sample rate was 10 000 s^{-1}, so that a complete transfer function spectrum (50 kHz and 100 points) was acquired in 10 ms. In order to correct for any shift of the VCO the extreme frequencies were measured with an HP5334B frequency meter via an IEEE-488 interface. Calibration of the dc rectified signals was achieved by applying the read level functions of the HP5334B to the amplified rf signals used for frequency measurement. AT-cut 10 MHz quartz crystals were employed [*International Crystal Manufacturing Company Inc., Oklahoma City, USA (cat. 31210),* 14 mm diameter, 0.168 mm thick with an active area of 0.196 cm^2]. The crystals were mounted in the cells by means of O-ring seals with only one face in contact with the electrolyte; this electrode was a common ground to both the ac and dc circuits.

3. Results and Discussion

3.1. RRDE and Chronopotentiometry

An initial study has shown that the presence of TTF in solution does not affect the oxygen reduction reaction (Fig. S.I.1). Fig. 1 depicts the cyclic voltammetry of a glassy carbon (GC) disk electrode in O_2 saturated 0.1 M $LiPF_6$/ DMSO containing 1 mM soluble TTF mediator.

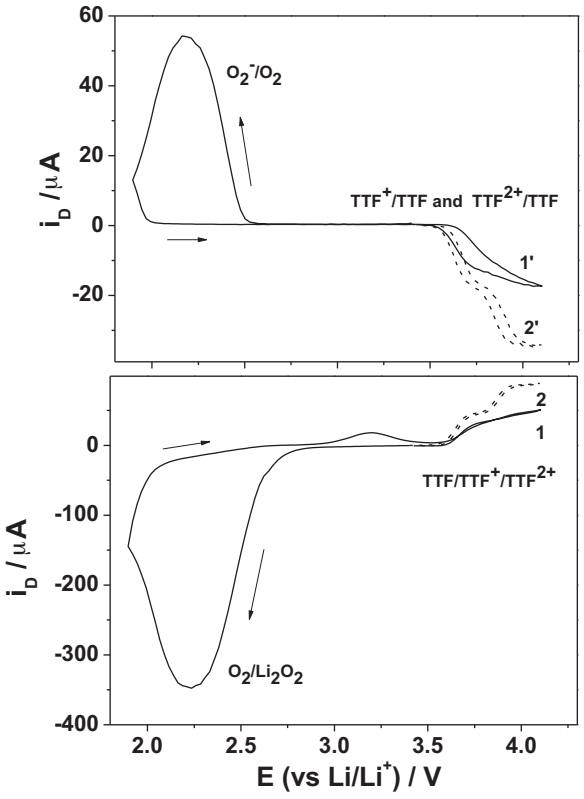

Fig. 1. GC disk (i_D) and Au ring current (i_R) CVs. vs. disk electrode potential (E) at W = 10 Hz in O_2 saturated $LiPF_6$ DMSO solution containing 1 mM TTF. Sweep rate 0.1 V. s^{-1}; E_R = 3.0 V. 1. First CV between 1.9 and 4.1 V, 2. Final CV after 50 oxidation-reduction cycles between 3.45 and 4.10 V.

If the potential limit is 3.45 V no electro-reduction of oxygen takes place and the two one-electron convective-diffusion waves of TTF oxidation are clearly seen (curve 2) while the ring electrode current displays the corresponding two one-electron waves for the reduction of TTF^+ and TTF^{2+} respectively (curve 2′). On the other hand, if the cathodic limit is extended to 1.9 V the O_2 reduction current rises from 2.85 V and a peak due to the formation of insoluble Li_2O_2 is clearly seen with surface passivation. The ring electrode in the collection mode of LiO_2 has a current maximum shifted to more reducing potentials with respect to the disk.

It should be noticed that in the reverse potential scan there is a small oxidation peak at the disk at 3.2 V which is attributed to Li_2O_2 oxidation [27] while there is no ring current until the disk reaches 3.5 V. At more positive potentials, however, TTF^+ oxidation at the disk and reduction of TTF^+ at the ring are hindered when the oxygen reduction potential was reached in a previous scan (compare curves 1 and 1′). This is due to the partial blocking of the surface by oxygen reduction products formed in the cathodic excursion to 1.9 V. If after reaching 1.9 V in the O_2 reduction region the potential range is limited to the TTF^+/TTF^{2+} reaction (3.45 to 4.1 V), the second oxidation wave to form TTF^{2+} on the surface is not seen in the first oxidation cycle, because TTF^+ is titrated not only by Li_2O_2 but also by decomposition products of $LiPF_6$ and solvent as has been shown by XPS [28]. However, in successive cycles the second wave progressively grows as these products are removed from the glassy carbon surface by a heterogeneous reaction with TTF^+ at the disk surface (see Fig. SI2).

Bruce and co-workers have shown the recharge of the Li-O_2 battery at 3.5 V in 10 mM TTF with DMSO containing lithium solution [16]; this is the potential range of TTF^+ formation. After continuous cycling in the potential range 3.45 and 4.10 V disk and ring currents approach the patterns expected for TTF/TTF^+ and TTF^+/TTF^{2+} fully developed waves (see curves 2 and 2′ in Fig. 1). Thus, at the disk electrode the blocking coverage decreases and the second wave at the ring electrode develops.

The removal efficiency of the disk blocking deposit by reaction with soluble TTF^+ was investigated by holding the potential at the positive limit, i.e. 4.10 V for different times (60 to 180 s) before recording the cyclic voltammetry. Total recovery of the cathodic oxygen reduction curve is achieved after 180 s of oxidation at 4.1 V and the current trace overlaps with that in the first scan (see Fig. S.I. 2).

Fig. 2 shows typical titration curves at a constant current of 25 μA cm^{-2} after a cathodic galvanostatic pulse in the ORR for 30 s in lithium solution with and without TTF. Notice that when TTF is not present in the solution the potential reaches high values which correspond to the solvent decomposition as has been shown by FTIR in situ experiment [15].

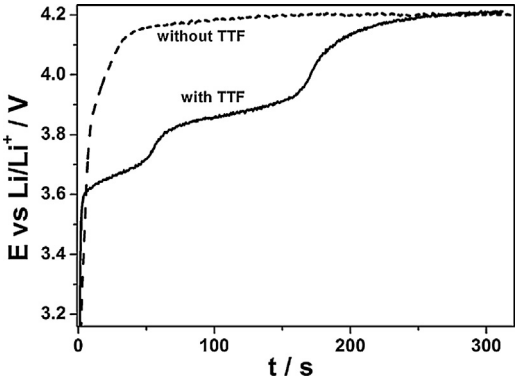

Fig. 2. Chronopotentiometry after 30 s of ORR with and without TTF present in solution.

However, with soluble TTF the curve presents two plateaux at 3.65 and 3.85 V which correspond to the TTF/TTF^+ and TTF^+/TTF^{2+} reactions.

This behaviour could be explained by the reaction of TTF^+ with the surface blocking deposit, which once eliminated causes the potential to change into the TTF^+ to TTF^{2+} oxidation process. Finally, when all the TTF^+ at the surface has been oxidized, the potential reaches the same high value as in the solution without TTF (Fig. 2).

3.2. AFM

In order to visualize the surface morphology, AFM measurement was carried out at flame annealed Au electrode with preferential (1 1 1) orientation after one second ORR at 2.05 V and after oxidation at 3.65 V in the presence and absence of soluble TTF. The morphology of the ORR products shows aggregates of nanocrystals with height never exceeding 20 nm in good agreement with previous reports [29]. After formation of the Li_2O_2 deposit the potential was stepped to 3.65 V during 60 s. In the absence of TTF in solution particles could still be observed and only at high potential, 4.35 V, all the surface deposit could be removed (see Fig. 3). With soluble TTF, on the other hand, the surface was almost recovered at 3.65 V in agreement with the battery performance reported by Bruce and co-workers [16].

3.3. EQCM

Further evidence of TTF^+ catalyzed removal of the blocking deposit by shuttling electrons to the underlying Au electrode was obtained with the EQCM as shown in Fig. 4A and B for 25 $\mu A\,cm^{-2}$ current pulses. Both the electrode potential and the areal mass time evolution are compared in the absence and in the presence of 1 mM TTF in solution during ORR and OER at respectively.

In the absence of the redox catalyst in solution, the oxidation starts close to the reversible potential of the O_2/Li_2O_2 redox couple, i.e. 2.96 V but a slow mass decreases never reaches the original level even at very high potential (4.5 V). With soluble TTF, on the other hand, a potential plateau at 3.6 V is reached with the same anodic current density. Titration of solid Li_2O_2 by TTF^+ takes place

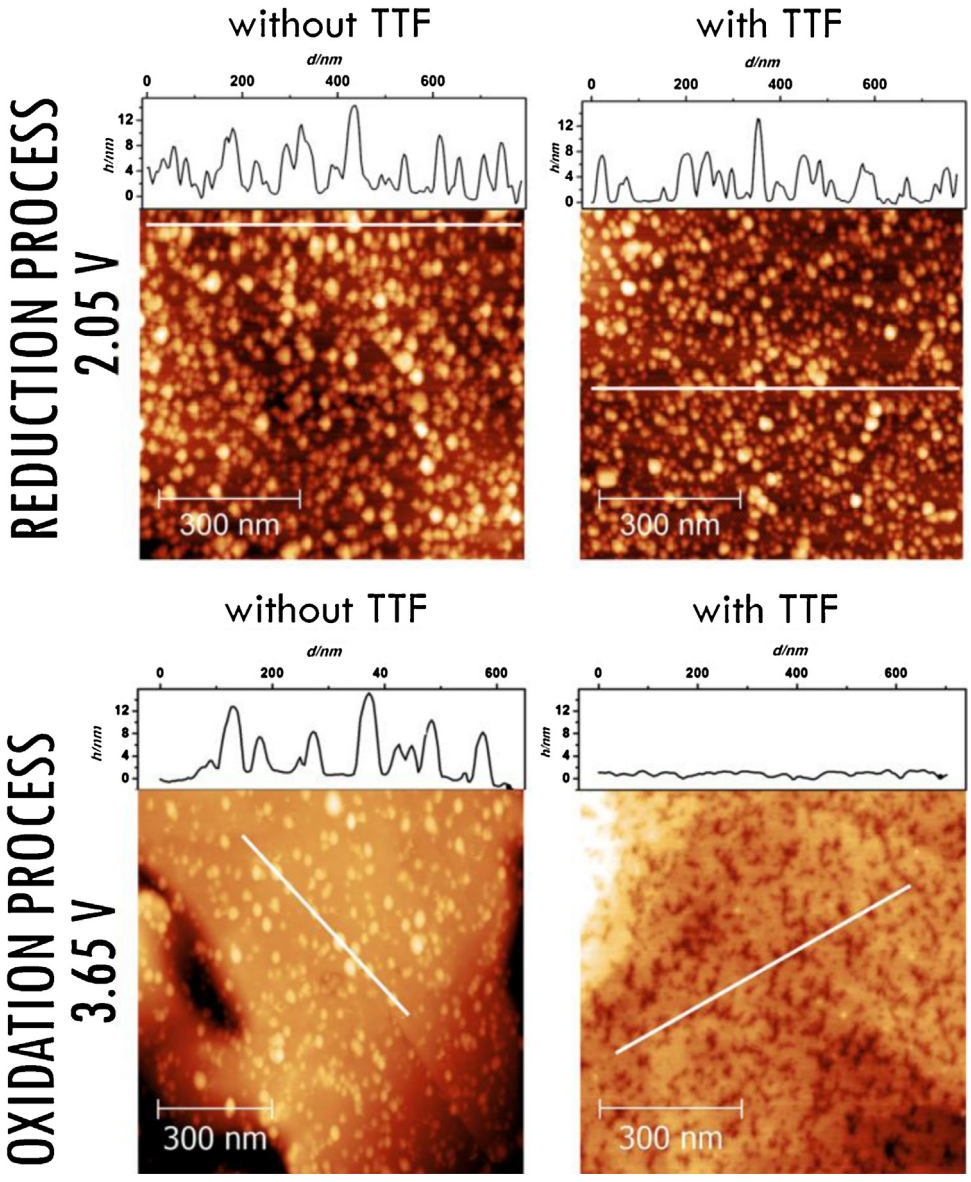

Fig. 3. AFM images of gold electrode covered with ORR products before (2.05 V) and after oxidation at 3.65 V.

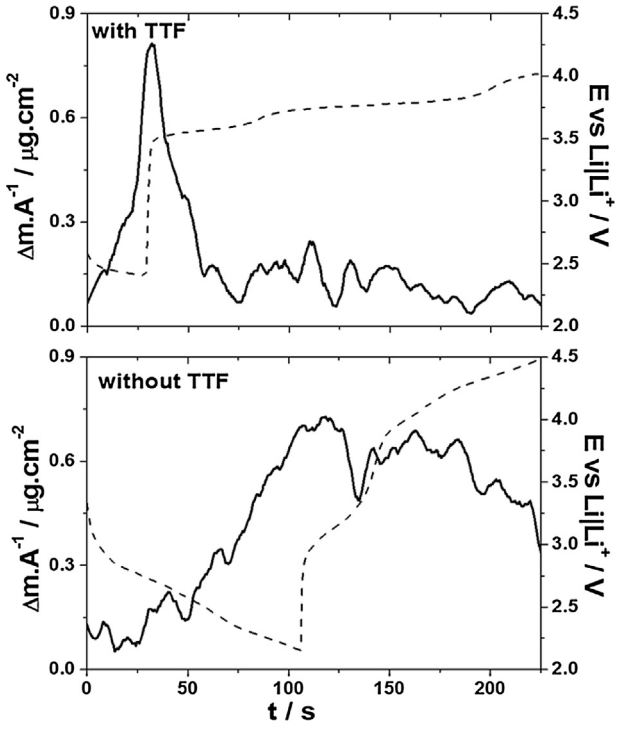

Fig. 4. EQCM experiment of 0.1 M $LiPF_6$ in DMSO with and without TTF in solution for 25 μA cm^{-2} current pulses.

according to:

$$Li_2O_2 + 2TTF^+ \rightarrow 2Li^+ + O_2 + 2TTF \quad (3)$$

which competes with the direct electrochemical oxidation:

$$Li_2O_2 \rightarrow O_2 + 2Li^+ + 2e \quad (4)$$

as the mass drops to the initial value and the TTF^+/TTF^{2+} sets the second plateau potential at 3.8 V.

Therefore the heterogeneous oxidation of Li_2O_2 by TTF^+ from solution is more effective than the direct electrochemical oxidation in the Li-O_2 cathode recharge below 4.0 V.

3.4. SECM

Finally, in order to demonstrate that TTF^+ acts as a chemical "pacman" by dissolving the blocking solid deposit on Au from the solution we have carried out SECM experiments in the generation-tip collection mode.

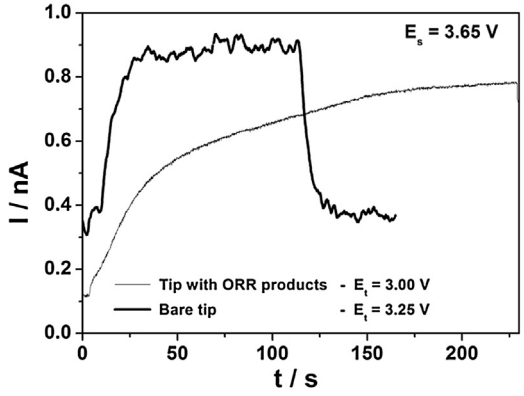

Fig. 5. Tip current vs time in SECM experiment of $LiPF_6$ in DMSO with 1 mM of TTF. Potential substrate (E_s) = 3.65 V.

In a control experiment in a 0.1 M $LiPF_6$ /DMSO solution containing TTF, the substrate was polarized at 3.65 V so that TTF^+ was generated and detected by electroreduction at the tip electrode polarized at 3.25 V (see Fig. 5). Then the tip electrode was polarized at 2.05 V during 2 minutes in order to block the surface with Li_2O_2 formed by the ORR (see Fig. S.I.3). The third step was to apply 3.65 V to the bare Au substrate while the tip was kept at 3.00 V (below Li_2O_2 oxidation potential) to detect TTF^+ by electroreduction. The TTF^+ generated at the Au substrate cannot be detected at the blocked tip unless this soluble redox catalyst oxidises de Li_2O_2 deposit blocking the tip.

Fig. 5 shows lower current at the passivated tip and a progressive enhancement of the current which is explained by removal of the solid blocking the tip by the TTF^+ generated at Au substrate, diffusing towards the tip electrode and titrating Li_2O_2.

4. Conclusions

We have studied the oxidation of Li_2O_2 and other ORR side products during the charging cycle of the oxygen cathode in $LiPF_6$/DMSO electrolyte by reaction with soluble TTF^+ using a variety of electrochemical techniques (RRDE, AFM, EQCM and SECM).

AFM examination of the surfaces before and after oxidation of Li_2O_2 shows that TTF^+ removes the solid blocking the electrode surface at lower potential than required for the electrochemical oxidation of DMSO to dimethyl sulfone.

SECM experiment demonstrates that soluble TTF^+ chemically reacts with surface species blocking the electrode consistent with EQCM mass recovery, RRDE and redox titration.

The experimental evidence demonstrates that soluble TTF^+ redox catalyst acts as a "chemical scavenger" by dissolving the blocking solid deposit on Au electrode decreasing the potential at which the oxygen cathode can be reoxidized so that the electrochemical oxidation of DMSO to dimethyl sulfone does not take place. Notice however that our XPS evidence shown elsewhere [28] demonstrates that ORR surface products react with DMSO and PF_6^- leading to spurious surface species which also contribute to the reoxidation overpotential unless TTF^+ acts on the surface.

Acknowledgements

Funding from CONICET and ANPCyT PICT 2012 No. 1452 and FS-Nano 07 and research doctoral and postdoctoral fellowships from CONICET by WRT, SEH and AYT, and from ANPCyT (M. del P) are gratefully acknowledged.

Appendix A. Supplementary data

Supplementary data associated with this article can be found, in the online version, at http://dx.doi.org/10.1016/j.electacta.2015.09.130.

References

[1] K.M. Abraham, Z. Jiang, A polymer electrolyte-based rechargeable lithium/oxygen battery, Journal of the Electrochemical Society 143 (1996) 1–5.
[2] P.G. Bruce, S.A. Freunberger, L.J. Hardwick, J.M. Tarascon, LigO2 and LigS batteries with high energy storage, Nature Materials 11 (2011) 19–29.
[3] J. Christensen, P. Albertus, R.S. Sanchez-Carrera, T. Lohmann, B. Kozinsky, R. Liedtke, J. Ahmed, A. Kojic, A critical review of Li/air batteries, Journal of the Electrochemical Society 159 (2012) R1–R30.
[4] L.J. Hardwick, P.G. Bruce, The pursuit of rechargeable non-aqueous lithium-oxygen battery cathodes, Current Opinion in Solid State and Materials Science 16 (2012) 178–185.
[5] C.O. Laoire, S. Mukerjee, K.M. Abraham, E.J. Plichta, M.A. Hendrickson, Influence of nonaqueous solvents on the electrochemistry of oxygen in the rechargeable lithium-air battery, Journal of Physical Chemistry C 114 (2010) 9178–9186.

[6] B.D. McCloskey, A. Speidel, R. Scheffler, D.C. Miller, V. Viswanathan, J.S. HummelshÃj, J.K. NÃrskov, A.C. Luntz, Twin problems of interfacial carbonate formation in nonaqueous Li-O 2 batteries, Journal of Physical Chemistry Letters 3 (2012) 997–1001.
[7] M.J. Trahan, Q. Jia, S. Mukerjee, E.J. Plichta, M.A. Hendrickson, K.M. Abraham, Cobalt phthalocyanine catalyzed lithium-air batteries, Journal of the Electrochemical Society 160 (2013) A1577–A1586.
[8] C.O. Laoire, S. Mukerjee, K.M. Abraham, E.J. Plichta, M.A. Hendrickson, Elucidating the mechanism of oxygen reduction for lithium-air battery applications, Journal of Physical Chemistry C 113 (2009) 20127–20134.
[9] M.M. Ottakam Thotiyl, S.A. Freunberger, Z. Peng, Y. Chen, Z. Liu, P.G. Bruce, A stable cathode for the aprotic Li-O2 battery, Nature Materials 12 (2013) 1050–1056.
[10] D. Xu, Z.L. Wang, J.J. Xu, L.L. Zhang, X.B. Zhang, Novel DMSO-based electrolyte for high performance rechargeable Li-O 2 batteries, Chemical Communications 48 (2012) 6948–6950.
[11] Y. Chen, S.A. Freunberger, Z. Peng, F. Barde, P.G. Bruce, Li-O-2 Battery with a Dimethylformamide Electrolyte, Journal of the American Chemical Society 134 (2012) 7952–7957.
[12] B.M. Gallant, D.G. Kwabi, R.R. Mitchell, J. Zhou, C.V. Thompson, Y. Shao-Horn, Influence of Li2O2 morphology on oxygen reduction and evolution kinetics in Li-O2 batteries, Energy and Environmental Science 6 (2013) 2518–2528.
[13] B.D. McCloskey, A. Valery, A.C. Luntz, S.R. Gowda, G.M. Wallraff, J.M. Garcia, T. Mori, L.E. Krupp, Combining accurate O2 and Li2O2 assays to separate discharge and charge stability limitations in nonaqueous Li-O 2 Batteries, Journal of Physical Chemistry Letters 4 (2013) 2989–2993.
[14] D. Sharon, M. Afri, M. Noked, A. Garsuch, A.A. Frimer, D. Aurbach, Oxidation of dimethyl sulfoxide solutions by electrochemical reduction of oxygen, Journal of Physical Chemistry Letters 4 (2013) 3115–3119.
[15] N. Mozhuzhukina, L.P. Mendez De Leo, E.J. Calvo, Infrared Spectroscopy Studies on Stability of Dimethyl Sulfoxide for Application in a Li-Air Battery, Journal of Physical Chemistry C 117 (2013) 18375–18380.
[16] Y. Chen, S.A. Freunberger, Z. Peng, O. Fontaine, P.G. Bruce, Charging a Li-O2 battery using a redox mediator, Nature Chemistry 5 (2013) 489–494.
[17] S. Schaltin, G. Vanhoutte, M. Wu, F. Bardé, J. Fransaer, A QCM study of ORR-OER and an in situ study of a redox mediator in DMSO for Li-O2 batteries, Physical Chemistry Chemical Physics 17 (2015) 12575–12586.
[18] M.J. Lacey, J.T. Frith, J.R. Owen, A redox shuttle to facilitate oxygen reduction in the lithium air battery, Electrochemistry Communications 26 (2013) 74–76.
[19] A.W. Lodge, M.J. Lacey, M. Fitt, N. Garcia-Araez, J.R. Owen, Critical appraisal on the role of catalysts for the oxygen reduction reaction in lithium-oxygen batteries, Electrochimica Acta 140 (2014) 168–173.
[20] L. Yang, J.T. Frith, N. Garcia-Araez, J.R. Owen, A new method to prevent degradation of lithium-oxygen batteries: Reduction of superoxide by viologen, Chemical Communications 51 (2015) 1705–1708.
[21] H.-D. Lim, H. Song, J. Kim, H. Gwon, Y. Bae, K.-Y. Park, J. Hong, H. Kim, T. Kim, Y. H. Kim, X. Lepro, R. Ovalle-Robles, R.H. Baughman, K. Kang, Superior Rechargeability and Efficiency of Lithium-Oxygen Batteries: Hierarchical Air Electrode Architecture Combined with a Soluble Catalyst, Angewandte Chemie-International Edition 53 (2014) 3926–3931.
[22] Y.G. Zhu, C. Jia, J. Yang, F. Pan, Q. Huang, Q. Wang, Dual redox catalysts for oxygen reduction and evolution reactions: Towards a redox flow Li-O2 battery, Chemical Communications 51 (2015) 9451–9454.
[23] D. Sun, Y. Shen, W. Zhang, L. Yu, Z. Yi, W. Yin, D. Wang, Y. Huang, J. Wang, D. Wang, J.B. Goodenough, A solution-phase bifunctional catalyst for lithium-oxygen batteries, Journal of the American Chemical Society 136 (2014) 8941–8946.
[24] K.M. Abraham, Lithium Batteries: Advanced Technologies and Applications, First ed., John Wiley and Sons, Inc., 2013.
[25] J.M. Tarascon, D. Guyomard, Li metal-free rechargeable batteries based on Li1 +xMn2O4 cathodes ($0 < x < 1$) and carbon anodes, Journal of the Electrochemical Society 138 (1991) 2864–2868.
[26] W.J. Albery, M.L. Hitchman, Current distribution on a rotating disc electrode, Transactions of the Faraday Society 67 (1971) 2408–2413.
[27] C.O. Laoire, S. Mukerjee, E.J. Plichta, M.A. Hendrickson, K.M. Abraham, Rechargeable lithium/TEGDME-LiPF6/O2 battery, Journal of the Electrochemical Society 158 (2011) A302–A308.
[28] F. Marchini, S.E. Herrera, W.R. Torres, A.Y. Tesio, F.J. Williams, E.J. Calvo, Langmuir 31 (33) (2015) 9236–9245.
[29] S.E. Herrera, A.Y. Tesio, R. Clarenc, E.J. Calvo, AFM study of oxygen reduction products on HOPG in the LiPF6-DMSO electrolyte, Physical Chemistry Chemical Physics 16 (2014) 9925–9929.